3454 J. Med. Chem. 2010, 53, 3454–3464
DOI: 10.1021/jm900232u

Journal of Medicinal Chemistry Article

Synthesis, Chiral High Performance Liquid Chromatographic Resolution and Enantiospecific Activity of a Potent New Geranylgeranyl Transferase Inhibitor, 2-Hydroxy-3-imidazo[1,2-*a*]pyridin-3-yl-2-phosphonopropionic Acid

Charles E. McKenna,*[,†] Boris A. Kashemirov,[†] Katarzyna M. Błażewska,[†] Isabelle Mallard-Favier,[†] Charlotte A. Stewart,[§] Javier Rojas,[§] Mark W. Lundy,[‡¶] Frank H. Ebetino,[‡¶] Rudi A. Baron,[∥] James E. Dunford,[⊥] Marie L. Kirsten,[∥] Miguel C. Seabra,[∥] Joy L. Bala,[†] Mong S. Marma,[†] Michael J. Rogers,[§] and Fraser P. Coxon*[,§]

[†]*Department of Chemistry, University of Southern California, Los Angeles, California 90089-0744,* [‡¶]*Procter & Gamble Pharmaceuticals, Mason, Ohio 45040,* [§]*Bone & Musculoskeletal Programme, Institute of Medical Sciences, University of Aberdeen, Aberdeen AB25 2ZD, U.K.,* [∥]*Molecular Medicine, National Heart and Lung Institute, Imperial College London, London SW7 2AZ, U.K., and* [⊥]*Nuffield Department of Orthopaedic Surgery, Oxford University, Institute of Musculoskeletal Sciences, Nuffield Orthopaedic Center, Headington, Oxford OX3 7LD, U.K.*

Received February 23, 2009

3-(3-Pyridyl)-2-hydroxy-2-phosphonopropanoic acid (3-PEHPC, **1**) is a phosphonocarboxylate (PC) analogue of 2-(3-pyridyl)-1-hydroxyethylidenebis(phosphonic acid) (risedronic acid, **2**), an osteoporosis drug that decreases bone resorption by inhibiting farnesyl pyrophosphate synthase (FPPS) in osteoclasts, preventing protein prenylation. **1** has lower bone affinity than **2** and weakly inhibits Rab geranylgeranyl transferase (RGGT), selectively preventing prenylation of Rab GTPases. We report here the synthesis and biological studies of 2-hydroxy-3-imidazo[1,2-*a*]pyridin-3-yl-2-phosphonopropionic acid (3-IPEHPC, **3**), the PC analogue of minodronic acid **4**. Like **1**, **3** selectively inhibited Rab11 vs. Rap 1A prenylation in J774 cells, and decreased cell viability, but was 33−60× more active in these assays. After resolving **3** by chiral HPLC (> 98% ee), we found that (+)-**3**-E1 was much more potent than (−)-**3**-E2 in an isolated RGGT inhibition assay, ∼17× more potent (LED 3 μM) than (−)-**3**-E2 in inhibiting Rab prenylation in J774 cells and >26× more active in the cell viability assay. The enantiomers of **1** exhibited a 4-fold or smaller potency difference in the RGGT and prenylation inhibition assays.

Introduction

Bisphosphonates are well-established antiresorptive drugs due to their ability to inhibit osteoclast-mediated bone resorption. Bisphosphonates also exhibit a range of other biological properties in vitro, including antitumor, antiparasitic, and antibacterial activities, raising the possibility of additional therapeutic uses in vivo.[1,2] The most potent bisphosphonate drugs currently used to treat bone metabolism disorders such as osteoporosis all contain an amino or other N-containing group (N-BPs) and have been shown to impede bone resorption by inhibiting farnesyl diphosphate synthase (FPPS), thereby blocking the synthesis of isoprenoid lipids required for the prenylation of small GTPases in osteoclasts.[2]

Phosphonocarboxylate (PC) analogues of N-BP drugs, e.g. 3-(3-pyridyl)-2-hydroxy-2-phosphonopropanoic acid (3-PEHPC, **1**), whose structure relates to the bone active drug 2-(3-pyridyl)-1-hydroxyethylidenebis(phosphonic acid) (risedronic acid, **2**; formulated as sodium risedronate), exhibit lower bone affinity than N-BPs but retain some ability to block protein prenylation.[3−6] However, PCs such as **1** selectively inhibit a different enzyme in the mevalonate pathway, Rab geranylgeranyl transferase (RGGT), thereby preventing prenylation of only the Rab family GTPases,[3,5] which are important regulators of organelle biogenesis and vesicle transport.[7] The SAR for inhibition of RGGT by PCs differs from that for inhibition of FPPS by N-BPs.[5] α-Halo and α-desoxy derivatives of **1** inhibit RGGT with similar potency to the parent PC, but α-halo and α-desoxy derivatives are generally weaker inhibitors of FPPS than **2** itself.[8,9]

Rab proteins such as Rab11 and Rab25 may contribute to the aggressiveness and progression of various cancers, including those that frequently metastasize to bone.[6,10] RGGT is overexpressed in a subset of human tumors, and there is evidence that the anticancer effects of some compounds designed as inhibitors of FPPS might involve suppression of prenylation mediated by RGGT,[11] stimulating interest in the design of specific inhibitors for this enzyme.[12] PC analogues of N-BP drugs exhibit antitumor properties in vitro, both by inhibiting cell invasion[13] and reducing cell viability,[4] and **1** has exhibited direct antitumor activity in an animal model.[14] **1** has only modest potency as an RGGT inhibitor, prompting a search for a more active analogues.

In this work, we describe the synthesis (6 steps) of 2-hydroxy-3-imidazo[1,2-*a*]pyridin-3-yl-2-phosphonopropionic acid (3-IPEHPC, **3**), which is the PC analogue of minodronic acid, **4**.[15] In contrast to the bisphosphonate **4**, the carbon bridging the two acidic groups **3** is chiral, raising the possibility of stereospecificity in its biological activity. The same achiral−chiral relationship exists between **2** and **1**. We have developed a method to resolve the **1** and **3** racemates using chiral HPLC, permitting individual evaluation of the component

*To whom correspondence should be addressed. For chemistry questions, contact CE McKenna (mckenna@usc.edu, Tel: +1-213-740-7007). For biology questions, contact FP Coxon (f.p.coxon@abdn.ac.uk, Tel: +44-1224-558974).

 Published on Web 04/15/2010

enantiomers.[16] In a companion study of the kinetics and mechanism of RGGT-mediated Rab geranylgeranylation, we found that (+)-**3** had significantly lower IC_{50} and *K*i values than **1** in inhibiting this enzyme.[17] We here compare the relative inhibitory potencies of the individual **3** and **1** stereoisomers in isolated RGGT, J744 cell viability and cellular prenylation assays, and also examine their selectivity vs. FPPS. The antiresorptive properties of **1** and **3** are examined using both in vitro (rabbit osteoclasts) and in vivo (Schenk) models (Chart 1).

Chart 1. Phosphonocarboxylic Acids 3-PEHPC (**1**) and 3-IPEHPC (**3**) and the Parent Bisphosphonic Acids, Risedronic Acid (**2**) and Minodronic Acid (**4**)

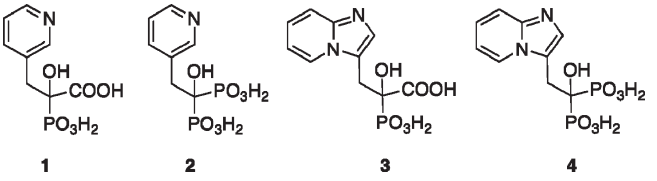

Results and Discussion

Synthesis of 3. The point of departure for our preparation of **3** was a constructive synthesis from the patent literature[18] in which condensation of aldehyde **6** with *N*,*N*-dimethylglycine ethyl ester followed by further transformations leads to the gateway enol **10**. However, our preliminary attempts to effect this initial condensation were unsuccessful, and we ultimately devised a new route to intermediate **10**, outlined in Scheme 1.

Our synthesis of **3** begins with a Vilsmeier−Haack formylation of imidazo[1,2-*a*]pyridine **5** to give the aldehyde **6**, following the approach of Almirante et al.[19] as modified by Gueiffier et al.[20] By washing the crude product with water, we were able to isolate clean **6** without chromatographic purification. In the next step, ethyl azidoacetate **7**, readily prepared from ethyl bromoacetate and sodium azide,[21] was condensed with **6** using sodium ethoxide dissolved in ethanol.[22] When following the original procedure,[22] the condensation was accompanied by an uncontrolled temperature rise with release of gas (possibly due to exothermic ethyl azidoacetate rearrangement[22]). This problem was circumvented by decreasing the equivalents of azide **7** from 10 to 4, as suggested by the preparation of the *t*-butyl esters of 2-azidocinnamate analogues where a smaller azide excess was successfully employed.[23] The reduction of **8** was effected, after some exploration of alternative conditions,[24] by hydrogenation over 10% Pd/C, giving the enamine product

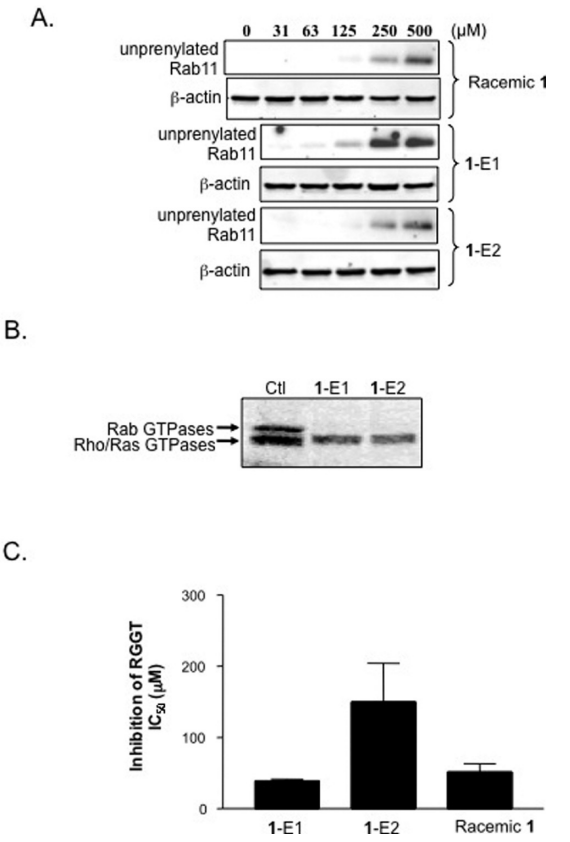

Figure 1. Enantiomers of **1** have small differences in activity. (A) Comparative effects of **1** and its enantiomers on Rab prenylation in J774 cells. Cells were treated for 24 h with 31−500 μM of the stereoisomers of **1**, or the racemate, then lysed in triton X-114 buffer and fractionated aqueous phases (containing unprenylated Rab proteins), electrophoresed and Western blotted for Rab11 or β-actin. (B) Selectivity of **1** enantiomers on GTPase prenylation. J774 cells were metabolically labeled for 18 h with [^{14}C]mevalonate, in the presence or absence of 1 mM compounds, then radiolabeled; prenylated GTPases were detected by phosphorimaging after separating proteins in cell lysates by electrophoresis. (C) Effect of **1** and its enantiomers on activity of RGGT in isolated enzyme assays, assessed by measuring the incorporation of [^{3}H]geranylgeranyl (from [^{3}H]GGPP) into Rab1a.

Scheme 1. Synthesis of 2-Hydroxy-3-imidazo[1,2-*a*]pyridin-3-yl-2-phosphonopropionic Acid, **3**

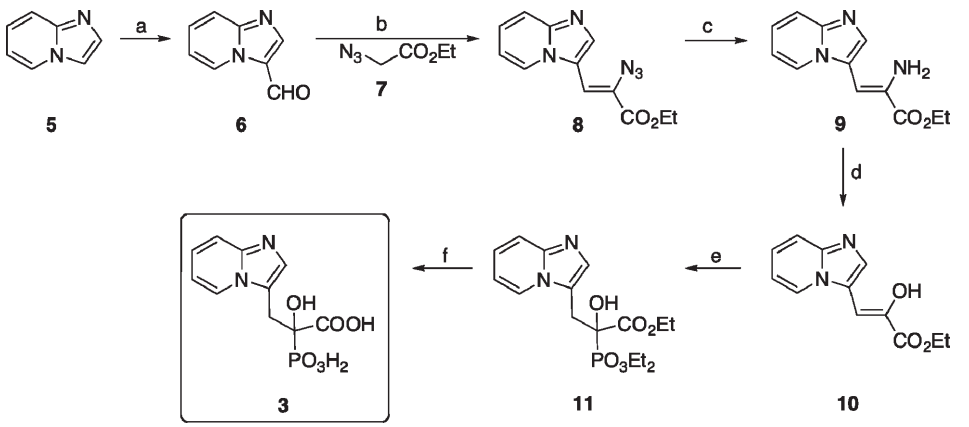

Reagents and conditions: (a) Vilsmeier reagent, from 2−140 °C, 31%; (b) EtONa/EtOH, from −30 °C to rt, 4 h, 55%; (c) H_2/10% Pd−C, MeOH, 2.5 h, rt, 100%; (d) AcOH/H_2O (7/1, v/v), 1.5 h, 0 °C, 59%; (e) $(EtO)_2P(O)H$, 70 °C, 21 h; (f) 6 N HCl, 6 h, reflux, 60%, (e) and (f) combined.

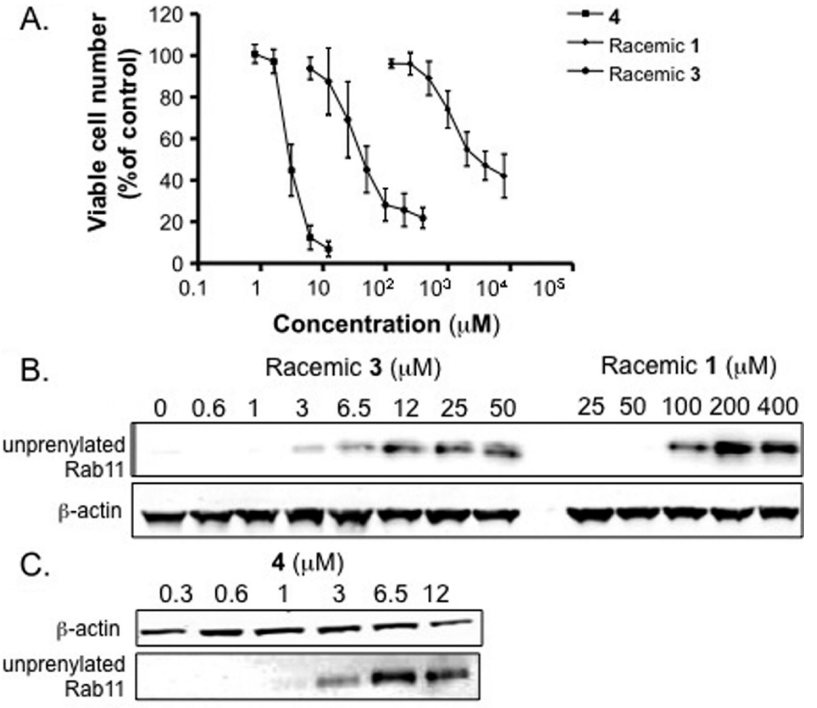

Figure 2. Compound **3** is a potent inhibitor of RGGT. (A) Effect of **4**, **1**, and **3** on J774 cell viability. Cells were treated with compounds for 48 h and then viable cell number assayed by Alamar blue assay (mean ± SEM; $n = 3$). (B,C) Effect of **4**, **1**, and **3** on Rab prenylation in J774 cells. The cells were treated for 24 h as indicated and then lysed in triton X-114 buffer and fractionated aqueous phases (containing unprenylated Rab proteins) were Western blotted for Rab11, or β-actin.

9 which was then hydrolyzed by treatment with 87% v/v acetic acid, providing the key intermediate **10**, in an overall yield of 10% (from **5**). A ^{1}H NMR study of this compound in $CDCl_3$ showed that $<1\%$ of the keto tautomer of **10**, ethyl 2-oxo-3-(imidazo[1,2-*a*]pyridin-3-yl)propanoate, was present, confirming the expected stabilization of the enol form by interaction with the extended π orbital system of the heterocycle. Addition of diethyl phosphite to **10** proceeded smoothly to provide the phosphonate adduct **11**, which however was found to be of limited stability due to rearrangement to its phosphate isomer. Phosphonate−phosphate rearrangements of α-hydroxy phosphonate diesters are well documented.[25] As a result, crude **11** was not purified but instead was quickly subjected to hydrolysis in refluxing concentrated hydrochloric acid, giving the acid **3**, which was isolated as a crystalline solid by precipitation and washing with ethanol and water. The compound was characterized by ^{1}H and ^{31}P NMR, HRMS, and elemental analysis.

Resolution of 1 and 3 Enantiomers. The role of chirality in the biological activity of bisphosphonate analogues has received little attention in the past. α,α-Disubstituted methylenebisphosphonate drugs such as **2**, zoledronate, alendronate, ibandronate, and clodronate are prochiral at the P−C−P carbon and have achiral substituents. We recently reported X-ray crystallographic evidence that [6,7-dihydro-5*H*-cyclopenta[*c*]pyridin-7-yl(hydroxy)-methylene]bis(phosphonic acid), an analogue of **2** incorporating a chiral bicyclic substituent, showed stereospecificity in forming its active site complex with FPPS.[26]

Unlike the bisphosphonates, all nonequivalently α,α-disubstituted phosphonocarboxylates have a chiral bridging α-carbon, but the relationship of this inherent stereoisomerism to their biological activities has remained unexplored. In search of a general method to resolve racemic PCs, we investigated separation on the commercially available quinine (ProntoSIL AX QN)−quinidine (ProntoSIL AX QD; the pseudoenantiomeric quinidine QD column has opposite chirality to the QN column) weak anion exchange HPLC columns introduced by Lindner et al.[27] Retention of the analyte by the stationary phase is believed to involve $\pi-\pi$ donor−acceptor, hydrogen bonding, and steric as well as ion-pairing interactions. Cinchona alkaloid-based columns have proved effective for the resolution of a number of different racemic monoacids[27] but have not been previously applied to multifunctional substrates such as **1** or **3**, which contain hydroxy- and nitrogen-containing heterocycle groups in addition to two different kinds of acid functionality with pK_as ranging from ~2 to ~7.

In preliminary studies using the QN column, we found that the peaks of the **1** or **3** enantiomers partially overlap and tail. One-pass separation gave the faster-eluting enantiomer (E1) with ~95% ee and the slowly eluting one (E2) with ~70−80% ee, as determined by reanalysis on QN and QD columns (the enantiomer with the shorter retention time on the QN column is dextrorotatory and is therefore referred to as (+)-**3**-E1 or (+)-**1**-E1, and the more slowly eluting, levorotatory enantiomer as (−)-**3**-E2 or (−)-**1**-E2; the order of elution is reversed on the QD column). Attempts to improve the enantioseparation by use of partial or full ester derivatives of the desoxy analogue of **1**, **13**, proved successful for its *P*,*P*-diester analogue **14** (see Supporting Information for details), but attempts to convert a **1** (or **3**) triester to its *P*,*P*-diester **15** under basic conditions led to rearrangement (to a phosphate ester). We therefore decided to concentrate on chiral HPLC reprocessing of the first-pass, enantiomer-enriched fractions obtained from the unmodified compounds. Because (−)-**3**-E2 elutes from the QN column within the tail of the faster-moving (+)-**3**-E1 peak, it was advantageous to carry out its second enrichment pass using the QD column

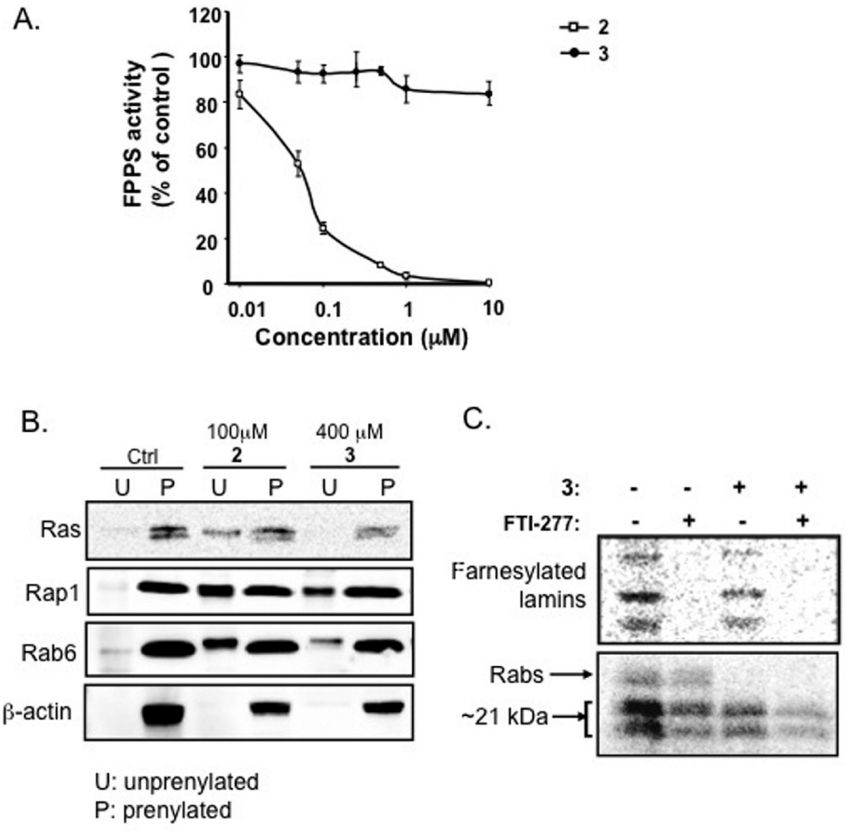

Figure 3. Compound **3** does not affect FPPS or protein farnesylation. (A) Assay for FPPS activity, in which partially purified recombinant human FPPS was preincubated with **2** or **3** for 10 min prior to commencing the assay by adding [^{14}C]IPP enzyme substrate. The data are the mean ± SEM (n = 4). (B) Effects of **2** and **3** on prenylation of Ras, Rap1, and Rab6 in J774 cells. The cells were treated for 24 h and then prenylated and unprenylated proteins separated by triton X-114 fractionation. Resulting aqueous (containing unprenylated proteins; U) and detergent-enriched (containing prenylated proteins; P) phases were then Western blotted for Ras, Rap1, Rab6, or β-actin. (C) Comparison of **18** and **3** prenylation selectivity in J774 cells. The cells were metabolically labeled for 18 h with [^{14}C]mevalonate, in the presence or absence of 400 μM **3** or 10 μM **18**, then radiolabeled; prenylated proteins were detected by phosphorimaging.

(on which it elutes first), whereas the (+)-**3**-E1-enriched fraction was rechromatographed on the original QN column. The %ee of each enantiomer was estimated to be ≥98% after two enrichment passes.

Biological Activity of 1 and 3 Stereoisomers

Stereoisomers of 1 Show Small Differences in Activity. The enantiomers of **1** show a relatively small difference in their ability to inhibit prenylation of Rab 11 in J774 cells, (+)-**1**-E1 being about four times as potent as (−)-**1**-E2 (LED ~63 vs. 250 μM, respectively) (Figure 1A). At 1 mM, both stereoisomers prevented the incorporation of [^{14}C] mevalonate into Rab GTPases, but not the Rho and Ras GTPases, confirming the specificity of these compounds for RGGT (Figure 1B). Neither (+)-**1**-E1 nor (−)-**1**-E2 affected the prenylation of Rap1A at concentrations up to 2 mM (data not shown). Consistent with these results, (+)-**1**-E1 was moderately more potent than isomer (−)-**1**-E2 in inhibiting incorporation of tritiated geranylgeranyl into Rab1a by isolated RGGT (IC_{50} values 39 ± 2.3 μM and 150 ± 54 μM, respectively; the racemate was of intermediate potency (IC_{50} 51.7 ± 11.5 μM) (Figure 1C).

Compound 3 Is a Potent Inhibitor of Rab Prenylation. (+)-**3** was previously shown to be ~25× more potent than **1** in inhibiting geranylgeranylation of Rab1a by isolated RGGT.[17] The greater potency of **3** was confirmed in a J774 cell viability assay (IC_{50} 47 μM compared to 2800 μM, respectively), although it is still less than that of its parent BP **4** (IC_{50} 3 μM; Figure 2A). Rab11 prenylation in J774 cells was ~30× more sensitive to **3** than to **1**, the LED of **3** (3 μM) being similar to that of minodronate itself, compared to ~100 μM for **1** (Figure 2B and C). The similarity between the potency of **3** and **4** for inhibition of Rab prenylation highlights the importance of inhibition of prenylation of non-Rab small GTPases in the mechanism of action of **4**, because this compound, which prevents the modification of all prenylated proteins, reduced J774 viability much more effectively than **3**. Moreover, the effect of **4** on protein prenylation is most likely exclusively the result of inhibition of FPPS because it has little effect on RGGT (IC_{50} > 1 mM; data not shown).

Similarly to **1**, **3** had almost no effect on FPP synthase activity at up to 10 μM (Figure 3A; note that the IC_{50} for the parent **4** is 3 nM in this assay[28]) and, unlike **2**, had no effect on the farnesylation of Ras at up to 400 μM (Figure 3B). Moreover, **3** prevented the incorporation of [^{14}C]mevalonate into Rabs but, unlike the specific FTase inhibitor FTI-277 (**18**),[29] did not affect farnesylation of nuclear lamins (Figure 3C). Therefore, like **1**, **3** is a selective RGGT inhibitor both in vitro and in whole cells but is significantly more potent. Interestingly, the difference in potency of the parent BPs (**4** vs. **2**) is only about 4-fold for both inhibition of FPPS and inhibition of prenylation (data not shown).

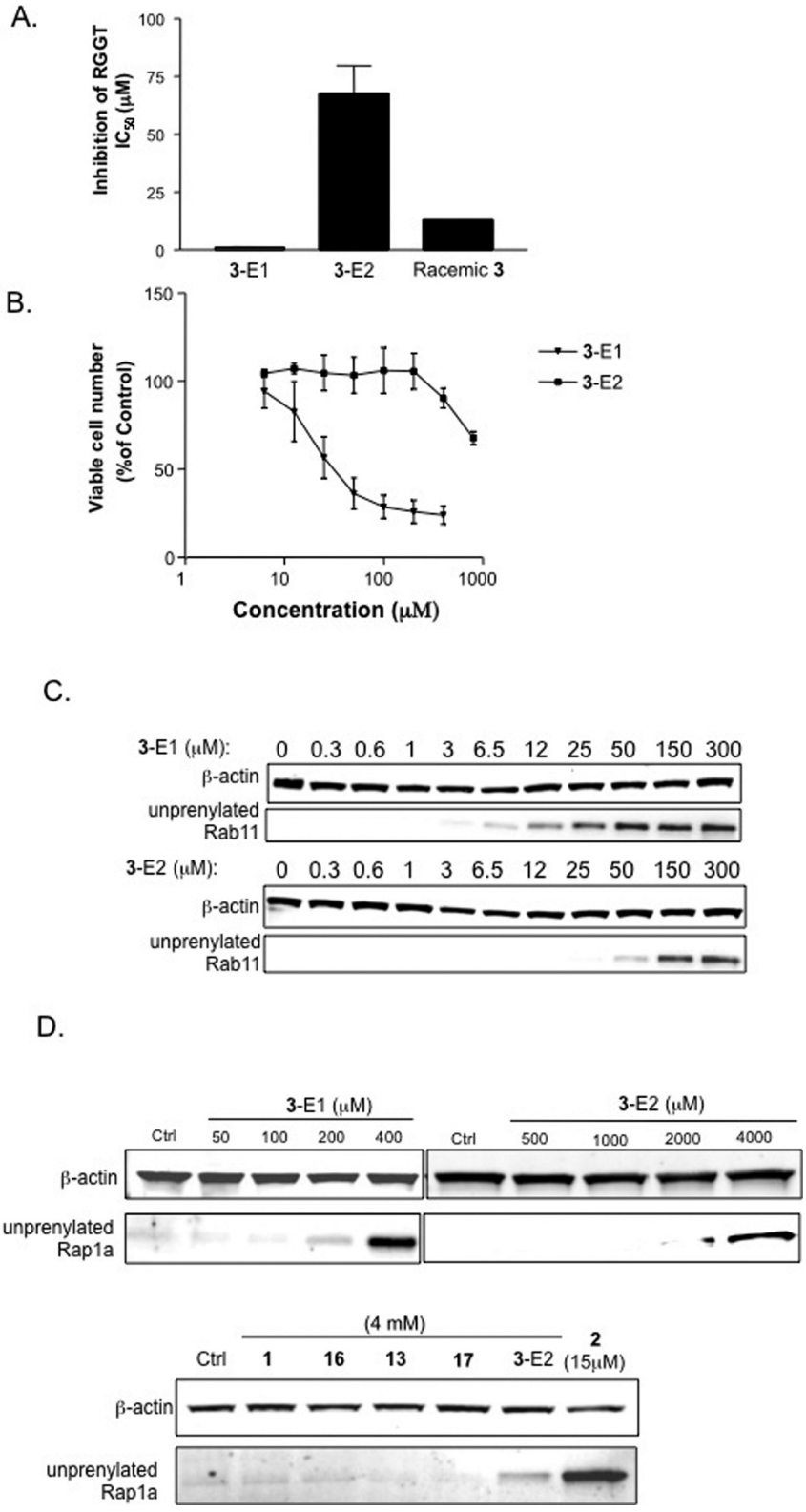

Figure 4. Isomers of **3** have differential activity. (A) The effect of **3** and its enantiomers on the activity of recombinant Rab GGTase in vitro was assessed by measuring the incorporation of [^{3}H]geranylgeranyl (from [^{3}H]GGPP) into Rap1A (mean ± SEM; n = 2). (B) Effects of **3** enantiomers on J774 cell viability. The cells were treated with the compounds for 48 h and then viable cell number assayed by Alamar blue assay (mean ± SEM; n = 3). (C,D) Effects of **3** enantiomers compared to **1**, **13**, **16**, and **17** on prenylation in J774 cells. Cells were treated for 24 h with the indicated concentrations (μM) of the compounds, then lysed in triton X-114 buffer and fractionated into aqueous phases (containing unprenylated Rab proteins) and Western blotted for unprenylated Rab11, β-actin, or unprenylated Rap1A.

Our finding that the desoxy analogue of **1** has reduced mineral affinity, but is of similar potency to **1**,[8] suggested that a similar modification to **3** could produce an equally potent Rab prenylation inhibitor with even lower affinity for bone. However, we have found that the desoxy analogue of **3** is less potent than **3** (data not shown).[9]

Chart 2. Structures of Compounds **13** and **16**−**19**

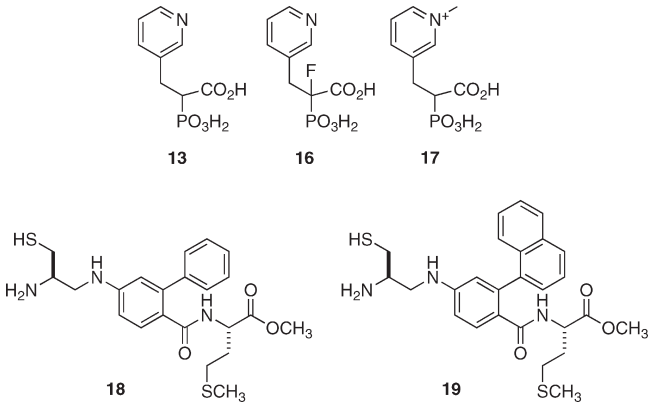

At a high concentration (400 μM), **3** appeared to have an additive effect with **18** in preventing the prenylation of ~21 kDa proteins (i.e., those modified by FTase and GGTase I), further indicating that **3** inhibits prenylation of *all* proteins modified with geranylgeranyl groups. In accordance, concentrations of ≥100 μM **3** also inhibited prenylation of proteins modified by GGTase I, such as Rap1 (Figures 3B and 4D). This suggests that at concentrations ~30 times higher than those necessary for inhibition of RGGT, **3** also weakly inhibits another enzyme of the mevalonate pathway downstream of FPPS, i.e., either GGPP synthase or GGTase I (discussed further in the section below concerning stereoisomers of **3**).

Stereoisomers of 3 Differ Markedly in Their Potencies. By contrast with **1**, stereoisomers of **3** show dramatically different activities, with (+)-**3**-E1 more potent than (−)-**3**-E2 in inhibiting RGGT (IC_{50} values 1.1 μM compared to 67.7 μM, respectively; Figure 4A). The racemate was of intermediate potency, although its IC_{50} appeared somewhat higher than might be expected from the (+)-**3**-E1 value. Large differences in potency were found with respect to reduction of J774 cell viability (IC_{50} values 31 μM for isomer (+)-**3**-E1 vs. > 800 μM for isomer (−)-**3**-E2; Figure 4B) and to a lesser extent, inhibition of Rab11 prenylation (LED ~3 and ~50 μM, respectively; Figure 4C). Similar to the racemate, (+)-**3**-E1 inhibited prenylation of Rap1A at concentrations around 30 times higher than those required for inhibition of Rab11 prenylation (~100 μM compared to ~3 μM). (−)-**3**-E2 also inhibited prenylation of Rap1A but only at a concentration ~80 times higher than that required for inhibition of Rab prenylation (Figure 4D). Other PC analogues, both active[8] (**1**, **13**, **16**) and inactive[3] (**17**) against RGGT, did not inhibit Rap1A prenylation even at this high concentration (4 mM) (Figure 4D). This indicates that the isomers of **3** are both able to inhibit an additional enzyme target besides RGGT (most likely GGPPS), but their potencies for inhibition of this enzyme are not directly related to their potencies for inhibition of RGGT (Chart 2).

The data demonstrate that (+)-**3**-E1 is the most potent selective PC inhibitor of RGGT yet to be identified. Other selective inhibitors of RGGT are similar in potency toward this enzyme in vitro (IC_{50} values 2.1−2.8 μM) but less effective in whole cell prenylation assays (inhibition of Rab prenylation at 20−50 μM).[12] Although the compound BMS-1 is a more potent inhibitor than (+)-**3**-E1 in enzyme assays, this compound is also a potent inhibitor of FTase.[11]

Compound 3 Likely Inhibits GGPP Synthase in Cells. Surprisingly, in isolated enzyme assays, (+)-**3**-E1 (and

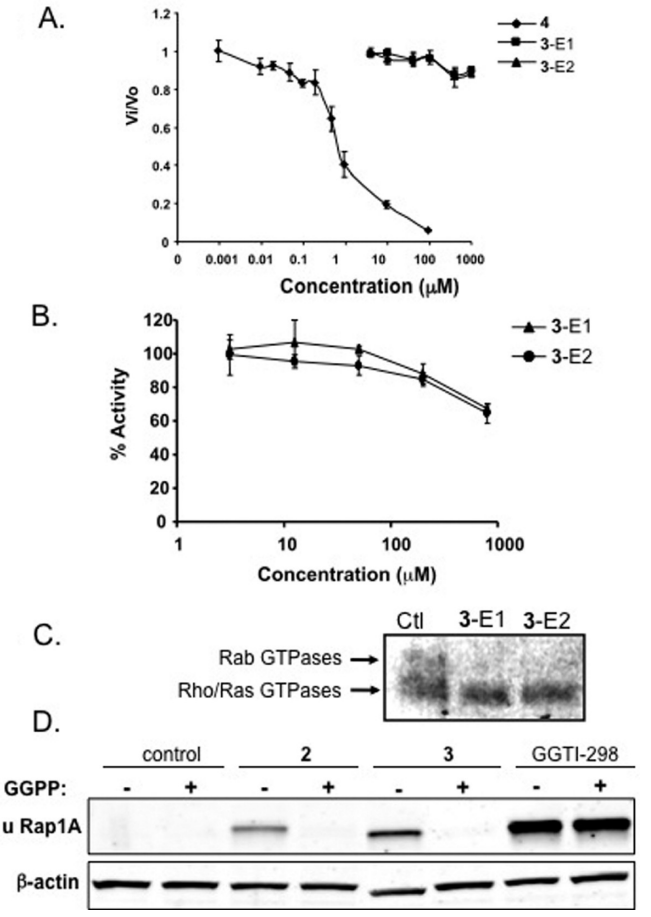

Figure 5. Compound **3** is a weak inhibitor of GGPPS in intact cells. (A) The effect of the enantiomers of **3** on activity of GGPPS in isolated enzyme assays (mean ± SEM; n = 3). (B) The effect of the enantiomers of **3** on activity of GGTase I in isolated enzyme assays (mean ± SEM; n = 3). (C) Selectivity of **3** enantiomers for inhibition of prenylation of GTPases in J774 cells. The cells were metabolically labeled for 18 h with [^{3}H]GGOH in the absence or presence of 400 μM (+)-**3**-E1 or (−)-**3**-E2 and then lysates separated by electrophoresis on 12% polyacrylamide-SDS gels and [^{3}H]-labeled, geranylgeranylated proteins detected by fluorography. (D) Effect of **2**, **3**, and **19** with/without added GGPP on Rap1A prenylation in J774 cells. Cells were treated for 24 h with 25 μM **2**, 400 μM **3** or 10 μM **19** in the presence or absence of 10 μM GGPP. Proteins in cell lysates were then separated by electrophoresis on 12% SDS/PAGE gels and unprenylated Rap1A (uRap1A) or β-actin detected by Western blotting.

indeed (−)-**3**-E2) had little effect on the activity of either GGPPS or GGTase I at concentrations up to 1 mM (Figure 5A and B). Despite these results, two pieces of evidence indicate that (+)-**3**-E1 achieves its effects on Rap1A prenylation through weak inhibition of GGPPS. First, (+)-**3**-E1 did not inhibit the incorporation of [^{3}H]GGPP into 21 kDa proteins (which are exclusive substrates for GGTase I; Figure 5C), indicating that this compound has no effect on GGTase I. Second, similar to **2**, the inhibition of prenylation of Rap1A caused by (+)-**3**-E1 could be overcome by the addition of GGPP, whereas the inhibition of Rap1A prenylation caused by the specific GGTase I inhibitor GGTI-298 (**19**)[30] was unaffected (Figure 5D). This indicates that (+)-**3**-E1 inhibits an enzyme upstream of GGTase I (i.e., GGPPS). It remains unclear why inhibition of GGPPS was so weak in isolated enzyme assays, but these differences could reflect differences in the relative concentrations of

Table 1. Effects of Selected PC and BP Analogues on Enzymes of the Mevalonate Pathway (Isolated Enzyme Assays), J774 Cell Viability, and Rab11 and Rap1A Prenylation[a]

compd	FPPS inhibition (IC_{50}, μM)	reduction of J774 viability (IC_{50}, μM)	RGGT inhibition (IC_{50}, μM)	inhibition of Rab11 prenylation LED (μM)	inhibition of Rap 1A prenylation LED (μM)	inhibition of GGPPS (IC_{50}, μM)	inhibition of GGTase 1 (IC_{50}, μM)
(±)-**1**	>1000[3]	2800	51.7	100	no effect at 4 mM	ND	>2000[b]
1-E1	ND	ND	39	63	no effect at 2 mM	ND	ND
1-E2	ND	ND	150	250	no effect at 2 mM	ND	ND
(±)-**3**	>10	47	12.5[c]	3	≥100	ND	ND
3-E1	ND	31	1.1[c]	3	100	>1000	>800
3-E2	ND	>800	67.7[c]	50	4000	>1000	>800
2	0.006[8]	31[8]	ND	12[b]	12[b8]	ND	ND
4	0.003[28]	3	>1000[b]	3[b]	3[b]	0.67	ND

[a] LED = lowest effective dose. ND = not determined. [b] Not shown in Figures. [c] Under the assay conditions of ref 17, IC_{50} values (Rab1a) of 1.3 and 32 μM were obtained for **3**-E1 and **1**, respectively. The K_i values (uncompetitive) obtained were 0.211 vs. 33.56 μM. The value for racemic **3** found here might be expected to be closer to that for **3**-E1. However, conservatively, the enantiomer IC_{50} ratio is at least ~20:1.

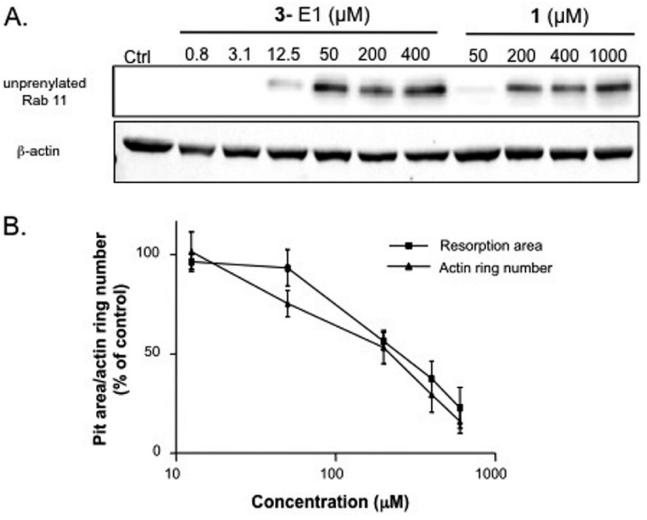

Figure 6. Compound **3** inhibits bone resorption by rabbit osteoclasts in vitro. (A) Rabbit osteoclasts were treated for 24 h, then lysed in triton X-114 buffer and aqueous phases (containing unprenylated Rab proteins) were Western blotted for Rab11 or β-actin. (B) Rabbit osteoclasts seeded onto dentine discs were treated with (+)-**3**-E1 for 48 h, then fixed, stained with TRITC-phalloidin, and the number of actin rings counted. Resorption pit area per disk was then determined by reflected light microscopy. Results are expressed as percentage of control and are the mean ± SEM of six independent experiments.

enzyme and substrates in the cells compared to the enzyme assays.

A summary of the biological activities of compounds **1**−**4**, **1**-E1-E2, and **3**-E1-E2 is presented in Table 1.

Compound 3 Inhibits Rab Prenylation in Osteoclasts but is a Weak Inhibitor of Bone Resorption. Compound **3** was much more potent (~15×) than **1** in inhibiting Rab prenylation in rabbit osteoclasts (effective at 12.5 μM compared to 200 μM for **1** (Figure 6A)). **3** was also an inhibitor of bone resorption (Figure 6B), but was only around 3-fold more potent than **1** in vitro (IC_{50} ~330 μM compared to 970 μM for **1**), and in vivo in the Schenk growing rat model (LED = 2.8 mg/kg compared to 12 mg/kg for **1**),[31] which may be somewhat less than anticipated from its potency for inhibiting Rab prenylation in osteoclasts. The in vivo data are for the racemates, thus the LED of the E-1 isomer of **3** should be lower, e.g. ~ 1.4 mg/kg. Unlike **1**, **3** affected the osteoclast cytoskeleton at concentrations that also inhibited resorption. The reason for the discrepancy between the effects of these two PCs on osteoclasts remains unclear.

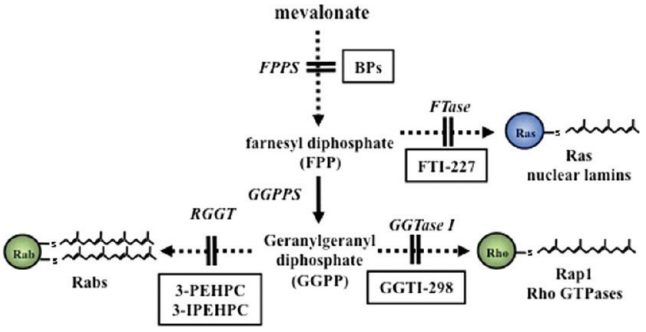

Figure 7. Mevalonate pathway, showing the prenylated proteins analyzed in this study and sites of action of inhibitors, including **1** (3-PEHPC) and **3** (3-IPEHPC). GGPPS is suggested as an additional site of action for **3**.

Conclusions

The novel PC analogue of minodronic acid, **3**, can be synthesized in six steps from imidazo[1,2-*a*]pyridine. As previously observed for a series of phosphonocarboxylate analogues of risedronate,[3,5,8] the structural modification of replacing one phosphonic acid group by a carboxylic acid group in the drug "backbone" of the parent N-BP drug redirects the active target from FPPS to RGGT, a more downstream enzyme of the mevalonate pathway, causing a selective inhibition of prenylation of Rab proteins (Figure 7).

Such compounds have potential therapeutic value, for example as antitumor agents, because Rab GTPases have been implicated in the pathogenesis of certain cancers that metastasize to bone.[6] In support of this, **1** has been shown to possess antitumor effects both in vitro[4,13] and in vivo.[14,32] The lower affinity of PCs for bone mineral[8] indicates that they are likely to be targeted to the bone microenvironment[5] but not as tightly associated with the bone surface as higher affinity BPs.

We have now demonstrated that **3** is a potent RGGT inhibitor compared to previously studied PCs and exhibits high selectivity for this enzyme. By separating chiral PC inhibitors into their component enantiomers for the first time, we have demonstrated that inhibition of RGGT can be highly dependent on analogue stereochemistry at the α-carbon and that almost all the activity of racemic **3** stems from one enantiomer [(+)-**3**-E1], which is the most potent PC-type selective RGGT inhibitor discovered to date. This compound illustrates the potential of bisphosphonate PC analogues as a new platform for drug design,[6] in addition to providing a new tool for investigating Rab-dependent biological processes.[3,5,33]

It will be of interest to cocrystallize RGGT[12] with the inhibitor **3** in complex, which we predict to show preferential binding of (+)-**3**-E1.

Experimental Section

General Methods, Reagents and Materials. Compounds **1** and **17** were gifts from Procter & Gamble Pharmaceuticals, Inc. Compounds **12**, **13**, and **16** were synthesized by our published method.[8] Synthesis of the partial esters of **13** (used for HPLC studies), **14**, and **15** is discussed in the Supporting Information. All solvents and reagents were reagent grade, purchased commercially and used without further purification, except as mentioned below. Phosphorus oxychloride and triethylamine were freshly distilled before use. HPLC were carried out using a Dynamax Rainin model SD-200 pump equipped with a Shimadzu SPD-10A VP UV−vis detector on ProntoSIL AX QN 8 mm × 150 mm and ProntoSIL AX QD 4 mm × 150 mm chiral columns (Bischoff Chromatography Leonberg, Germany). Columns were eluted isocratically with 0.7 M TEAAc containing 75% MeOH at pH 5.8 for enantioseparation of **3**, or with 0.25 M TEAAc, 75% MeOH at pH 6.9 for enantioseparation of **1**. Optical rotations for both enantiomers of **3** dissolved in water at pH 6.3 were determined on a Jasco P-2000 polarimeter, cell path length 10 cm. NMR spectra were measured on a Varian Mercury 400 spectrometer. Chemical shifts (δ) are reported in parts per million (ppm) relative to internal residual $CHCl_3$ in $CDCl_3$ (δ 7.29), or internal residual HDO in D_2O (pH ~12, δ 4.8). Elemental analysis of racemic **3** was performed by Gallbraith Laboratories Inc., Knoxville, TN. HRMS analysis was performed at the UC Riverside, MS Laboratory, using a VG-ZAB MS spectrometer in FAB mode. UV spectra were measured on a Beckmann Coulter DU 800 spectrophotometer. Concentrations of **3** enantiomers in aqueous solution (pH 6.3) were assigned by UV, using ε = 6450 at 280 nm.

For biological assays, PC compounds were dissolved in PBS, the pH was adjusted to 7.4 with 1 M NaOH, and the solution filter-sterilized before use. Antibodies used for immunoblotting were: antiunprenylated Rap1A (sc-1482) from Santa Cruz Biotechnology, anti-Rab11 (05−853) from Upstate Serologicals (Lake, Placid, NY), and β-actin from Sigma (Poole, UK). 23c6 antivitronectin receptor (VNR) antibody was a generous gift of Prof. Mike Horton (University College London, UK). [^{3}H]-GGOH was obtained from American Radiochemicals Ltd. (St Louis, MO). [^{14}C]Mevalonic acid lactone, Enhance reagent, and [1-^{3}*H*]*trans*-geranylgeranyl pyrophosphate (GGPP) were purchased from NEN (Hounslow, UK). Solvent was removed from [^{3}H]GGOH and [^{14}C]mevalonic acid lactone by evaporating in nitrogen. All other reagents were from Sigma Chemical Co (Poole, UK) unless stated otherwise.

Imidazo[1,2-*a*]pyridin-3-carbaldehyde (6).[19,20] To DMF (120 mL, 1.55 mol) cooled to 2 °C, freshly distilled phosphorus oxychloride (61 mL, 0.65 mol) was slowly added. The temperature was allowed to gradually rise to room temperature. After recooling to 2 °C and a solution of imidazo[1,2-*a*]-pyridine **5** (10 g, 0.085 mol) in DMF (60 mL) was added dropwise. The mixture was warmed to 105 °C, and the temperature rose to 140 °C. The oil bath was removed until the temperature stabilized at 120 °C. Heating was then continuted for 45 min at 120 °C and 2.5 h at 85 °C. After cooling, the reaction mixture was poured into 5% HCl (600 mL) cooled by a water bath and then brought to pH 9 by adding 20% aq NaOH. The resulting solution was extracted with CH_2Cl_2 (1200 mL) overnight. The organic layer was separated and dried over $MgSO_4$, the solvent removed under reduced pressure, and the crude product washed with water (5 × 15 mL) and dried: 3.49 g (31%) of a white solid was obtained. ^{1}H NMR ($CDCl_3$): 7.17 (dt, $^3J_{HH}$ = 6.80 Hz, $^4J_{HH}$ = 0.8 Hz, CH, 1H), 7.60 (ddd, $^3J_{HH}$ = 8.40, 6.80 Hz, $^4J_{HH}$ = 1.6 Hz, CH, 1H), 7.83 (m, CH, 1H), 8.35 (s, CH, 1H), 9.53 (m, CH, 1H), 9.98 (s, CHO, 1H) (for a discussion of the ^{1}H NMR of imidazo[1,2-*a*]pyridine analogues, see Paudler and Blewitt[34]).

Ethyl Azidoacetate (7).[21] To a cooled (0−5 °C) solution of ethyl bromoacetate (40 g, 0.24 mol) in 250 mL of acetone, a solution of sodium azide (38.9 g, 0.60 mol) in 200 mL of water was added dropwise. The temperature was increased to 63 °C and maintained at that temperature for 4 h. The reaction mixture was then cooled to room temperature and extracted with CH_2Cl_2 (7 × 70 mL). The combined extracts were washed with saturated $NaHCO_3$ (3 × 40 mL) and water (3 × 20 mL) and dried over $MgSO_4$. Solvents were evaporated under reduced pressure, and the residue was dried under vacuum. The product was obtained as a colorless oil in 96% yield (29.9 g). ^{1}H NMR, $CDCl_3$: 1.36 (t, $^3J_{HH}$ = 6.80 Hz, CH_3, 3H), 3.92 (s, CH_2N_3, 2H), 4.31 (q, $^3J_{HH}$ = 6.80 Hz, CH_2, 2H).

(*Z*)-2-Azido-3-imidazo[1,2-*a*]pyridin-3-yl-acrylic Acid Ethyl Ester (8).[22] To ethanolic sodium ethoxide, generated by the addition of metallic sodium (4.5 equiv) to ethanol (140 mL) and cooled to −30 °C, a solution of aldehyde **6** (4 g, 0.0273 mol) and ethyl azidoacetate **7** (14.1 g, 0.109 mol) in ethanol (120 mL) was added dropwise. The temperature was slowly increased to room temperature, and the mixture allowed to stand for 4 h. The reaction was quenched with a saturated aqueous solution of NH_4Cl (360 mL) and extracted with diethyl ether (1200 mL). The combined organic extracts were dried over Na_2SO_4 and concentrated in vacuo. The crude product was chromatographed on silica gel, eluted with EtOAc:hexane (3:2), giving a yellowish solid (3.87 g, 55%). Stereochemical assignment follows Chezal et al.[22] ^{1}H NMR $CDCl_3$: 1.45 (t, $^3J_{HH}$ = 7.2 Hz, CH_3, 3H), 4.44 (q, $^3J_{HH}$ = 7.2 Hz, CH_2, 2H), 7.00 (dt, $^3J_{HH}$ = 7.0, $^4J_{HH}$ = 0.8, CH, 1H), 7.12 (s, CH=, 1H), 7.35 (ddd, $^3J_{HH}$ = 8.8, 7.0, $^4J_{HH}$ = 1.2, CH, 1H), 7.73 (bd, $^3J_{HH}$ = 8.8, CH, 1H), 8.24 (d, $^3J_{HH}$ = 7.0, CH, 1H), 8.54 (s, CH, 1H).

(*Z*)-2-Amino-3-imidazo[1,2-*a*]pyridin-3-yl-acrylic Acid Ethyl Ester (9). A mixture of azide **8** (4.63 g, 0.018 mol) and 10% palladium on charcoal (1.05 g) in methanol (130 mL) was stirred under H_2 for 2.5 h at rt. The reaction progress was controlled by TLC (CH_2Cl_2/acetone 9:1). The reaction mixture was filtered and the filtrate concentrated under reduced pressure. The product was obtained quantitatively (4.15 g). ^{1}H NMR, $CDCl_3$: 1.42 (t, $^3J_{HH}$ = 6.80 Hz, CH_3, 3H), 4.37 (q, $^3J_{HH}$ = 6.80 Hz, CH_2, 2H), 6.61 (s, CH=C, 1H), 6.92 (dt, $^3J_{HH}$ = 6.80 Hz, $^2J_{HH}$ = 1.2 Hz, CH, 1H), 7.26 (ddd, $^3J_{HH}$ = 6.80 Hz, 10.0 Hz, $^2J_{HH}$ = 1.2 Hz, CH, 1H), 7.66 (m, CH, 1H), 7.87 (s, CH, 1H), 8.15 (m, CH, 1H).

(*Z*)-2-Hydroxy-3-imidazo[1,2-*a*]pyridin-3-yl-acrylic Acid Ethyl Ester (10). A solution of enamine **9** (3.5 g, 0.015 mol) in acetic acid (5 mL) and water (35 mL) was stirred for 1.5 h at 0 °C. A solid precipitated. The mixture was concentrated in vacuo, and the semisolid residue was washed with water and dried in vacuo, leaving the product as an off-white solid (2.08 g, 59%). ^{1}H NMR: 1.43 (t, $^3J_{HH}$ = 7.20 Hz, CH_3, 3H), 4.42 (q, $^3J_{HH}$ = 7.20 Hz, CH_2, 2H), 6.78 (s, CH=C, 1H), 6.96 (dt, $^3J_{HH}$ = 6.80 Hz, $^2J_{HH}$ = 1.2 Hz, CH, H), 7.26 (m, CH, 1H), 7.72 (d, $^3J_{HH}$ = 9.20 Hz, CH, 1H), 8.22 (d, $^3J_{HH}$ = 6.80 Hz, CH, 1H), 8.32 (s, CH, 1H).

2-(Diethoxyphosphoryl)-2-hydroxy-3-imidazo[1,2-*a*]pyridin-3-yl-propionic Acid Ethyl Ester (11). A mixture of enol **10** (1.45 g, 0.006 mol) in diethyl phosphite (25 mL) was stirred for 21 h at 70 °C. After cooling, it was concentrated in vacuo and subjected to hydrolysis without further isolation or purification due to its instability. ^{1}H NMR, $CDCl_3$: 1.40, 1.42, 1.43 (3t, $^3J_{HH}$ = 6.80 Hz, 3CH_3, 9H), 3.62 (dd, $^2J_{HH}$ = 16.00, $^3J_{HP}$ = 6.80 Hz, CH, 1H), 3.84 (dd, $^2J_{HH}$ = 16.00, $^3J_{HP}$ = 4.40 Hz, CH, 1H), 4.18−4.34 (m, 3CH_2O, 6H), 6.87 (t, $^3J_{HH}$ = 6.80 Hz, CH, 1H), 7.22−7.26 (m, CH, 1H), 7.48 (s, CH, 1H), 7.68 (d, $^3J_{HH}$ = 8.80 Hz, CH, 1H), 8.38 (d, $^3J_{HH}$ = 7.20 Hz, CH, 1H).

2-Hydroxy-3-imidazo[1,2-*a*]pyridin-3-yl-2-phosphonopropionic Acid (3). A solution of the crude ester **11** in concentrated

hydrochloric acid (45 mL) was refluxed for 5 h. After evaporation under reduced pressure, the residue was dissolved partially in 100 μL of water and precipitated by addition of ethanol (50 mL). The precipitate was filtered, washed with water (500 μL) and then ethanol (40 mL), filtered, washed again with ethanol, and dried, giving an off-white solid (1.03 g, 60% from **10**). Two overlapping peaks of approximately equal area on an AX QN HPLC column (see below). ^{1}H NMR (D_2O, pH 12.8): 3.35 (dd, $^2J_{HH}$ = 15.6, $^3J_{HP}$ = 7.2, CHHCP, 1H), 3.75 (dd, $^2J_{HH}$ = 15.6, $^3J_{HP}$ = 1.2, CHHCP, 1H), 6.90 (t, $^3J_{HH}$ = 6.4, CH, 1H), 7.26 (bdd, $^3J_{HH}$ = 9.2, 6.4, CH, 1H), 7.35 (s, CH, 1H), 7.45 (d, $^3J_{HH}$ = 9.2, CH, 1H), 8.41 (d, $^3J_{HH}$ = 6.4, CH, 1H). ^{31}P NMR (D_2O, pH 12.8): 15.06. ^{13}C NMR (D_2O, pH 12.8): 29.30 (CH_2CP), 80.51 (d, $^1J_{CP}$ = 138.3, CP), 112.10, 115.40 (2s, 2CH), 122.93 (d, $^3J_{CP}$ = 16.8, C), 125.26 (s, 2CH), 130.07 (s, CH), 145.12 (s, C), 179.55 (s, C=O). Anal. Calcd for $C_{10}H_{11}N_2O_6P(H_2O)_2$-$(C_2H_5OH)_{0.16}$: C 37.61%, H 4.88%, N 8.50%. Found: C 37.44%, H 5.00%, N 8.63%. HRMS for $C_{10}H_{10}N_2O_6P^-$ (m/z): found 285.0283; calcd: 285.028.

Separation of 3 Enantiomers by Chiral HPLC. 3 was eluted isocratically on a ProntoSIL AX QN column (8 mm × 150 mm) with 0.7 M triethylamine/acetic acid containing 75% MeOH at pH 5.8. Each injection was done using 5−7 mg of **3**, which was dissolved in 100 μL buffer and TEA at pH 6.7. The two fractions corresponding to partially overlapping peaks were separated and evaporated under reduced pressure. During the evaporation process in glass vessels, but not in plastic (PP) vessels, an adduct sometimes forms in variable amounts (2−10%), detectable by chiral HPLC and ^{31}P NMR analysis, that reverts (without racemization) to **3** (E1 or E2) on treatment with water at pH 7−8 (Supporting Information). The origin and structure of this compound will be discussed elsewhere.[35] On the basis of reanalysis using QN and QD columns, the %ee of the enantiomer fraction with the shorter retention time, (+)-**3**-E1, was about 95%. The enantiomer with the longer retention time, (−)-**3**-E2 was obtained in about 70−80% ee. The fraction enriched with (+)-**3**-E1 was further purified using the same ProntoSIL AX QN column, whereas the fraction enriched in (−)-**3**-E2 was repurified using a ProntoSIL 4 mm × 150 mm AX QD column, which reversed the elution order, eliminating tailing of (+)-**3**-E1 into (−)-**3**-E2. The enantiomeric purity of both enantiomers was ≥98%, defined by chiral HPLC using the ProntoSIL AX QN and AX QD columns to define the %ee of (−)-**3**-E2 and (+)-**3**-E1, respectively. The optical rotations of the two enantiomers were opposite, as expected:

$$(+)\text{-}\mathbf{3}\text{-E1} : [\alpha]_D^{23} = +112.4 \pm 0.2 \; (c = 0.68\text{g/dL}, H_2O, \text{pH } 6.3)$$

$$(-)\text{-}\mathbf{3}\text{-E2} : [\alpha]_D^{23} = -110.9 \pm 0.2 \; (c = 0.64\text{g/dL}, H_2O, \text{pH } 6.3)$$

Determination of the Extinction Coefficient of 3. First, UV spectra of racemic **3** in aqueous solutions at pH 9, 7, 5, and 3 were acquired, which displayed an isosbestic point at 296 nm between pH 9 and pH 7. The extinction coefficient determined for pure racemic **3** (a sample which passed elemental analysis and was pure by ^{31}P, ^{1}H, ^{13}C NMR; MW = 286.2) in 0.1 N phosphate buffer, at pH 6.3 was 6450 ± 3 at 280 nm (λ_{max}) (n = 3).

RGGT and GGTase I Assays. RGGT activity was measured by determining the incorporation of [^{3}H]GGPP into His-tagged canine Rab1a protein as previously described.[36] The final concentrations in the prenylation reaction were 50 mM sodium HEPES, pH 7.2, 5 mM $MgCl_2$, 1 mM DTE, 1 mM NP-40, 4 μM Rab1a, 5 μM GGPP (800 dpm/pmol), 2 μM REP-1, and 50 nM RGGT. All reactions were allowed for 30 min at 37 °C in a 25 μL volume in glass tubes (Fisher). The assay was conducted in duplicate and repeated in three independent reactions. The experimental data were fitted using the enzyme kinetic module from Systat Software and are expressed as mean ± SEM of three independent experiments.

FPPS and GGPPS Assays. FPP synthase and GGPP synthase were purified and assayed as described.[37] Briefly, compounds under investigation were preincubated with 1 pmol FPPS or 6 pmol GGPPS for 10 min and then the reaction initiated by adding 20 μL of substrate containing 50 μM [1-^{14}C]IPP (4 μCi/mmol) and either 50 μM GPP for FPPS or 50 μM FPP for GGPPS. After 5 min, the assay was terminated by adding 200 μL of 1:4 conc HCl/methanol. Reaction products were then extracted with 0.5 mL of scintillation fluid (Microscint E, Perkin-Elmer) and radioactivity in the upper phase determined by scintillation counting. Data was analyzed using Graphpad Prism.

Assessment of Rab Prenylation by Western Blotting. The effects of the compounds on protein prenylation were studied using triton X-114 fractionation in which prenylated proteins partition into the detergent-rich phase, whereas unprenylated proteins remain in the aqueous phase.[5] Briefly, cells were treated for 24 h, then lysed in 20 mM Tris, 150 mM NaCl, pH 7.5, 1% Triton X-114, a sample taken for determination of protein concentration, and then remaining lysate incubated at 37 °C for 10 min. Following centrifugation at 13000g for 2 min, the aqueous and detergent-rich phases were separated and then Triton X-114 added back to the aqueous phase to 1% v/v and the extraction process repeated. Aqueous phases, equivalent to 20 mg of unfractionated lysate, were electrophoresed on 12% gels and Western blotted for Rab11 (an abundant, ubiquitous Rab), β-actin, or unprenylated Rap1A. Effects are expressed as the lowest effective dose (from 3 independent experiments), i.e., the lowest dose at which unprenylated Rap1A or Rab11 was detected.

In some cases in which prenylation of Rap1A was assessed, cells were lysed simply in RIPA buffer[38] because the antibody recognizes only the unprenylated form of Rap1A and therefore fractionation is not required.

Cell Viability Assay. The number of viable J774 cells following treatment with the compounds for 48 h was assessed as previously described.[3] Experiments were carried out in replicates of 6 and the data expressed are the mean ± SEM of at least four independent experiments.

Incorporation of [^{14}C]Mevalonate and [^{3}H]GGOH into Prenylated Proteins in Intact Cells. Detection of prenylated proteins in J774 macrophages was carried out as described previously.[3] Briefly, cells were depleted of mevalonate by incubation with 5 μM mevastatin for 4 h and then transferred into fresh medium containing 5 μM mevastatin and either 7.5 μCi/mL [^{14}C]mevalonic acid lactone or 30 mCi/mL [^{3}H]GGOH plus compounds under investigation. After 18 h, the cells were lysed in RIPA buffer and then 50 μg of cell lysate from each treatment were electrophoresed on 12% polyacrylamide-SDS gels under reducing conditions. After electrophoresis, the gels were fixed in 10% (v/v) acetic acid, 40% (v/v) methanol, 50% (v/v) distilled water, and then [^{14}C]-labeled gels were dried and labeled proteins visualized on a BioRad personal FX imager after exposure to a Kodak phosphorimaging screen. [^{3}H]-Labeled gels were incubated in Enhance for 30 min prior to drying. [^{3}H]-Labeled proteins were then visualized by exposing the gel to preflashed Hyperfilm-MP (Amersham, Aylesbury, UK) for 6 days at −70 °C.

Rabbit Osteoclast Cultures. Mature osteoclasts were isolated from 2-day old New Zealand White rabbits as previously described[39] and partially purified through an FCS gradient. Cells were then resuspended in fresh a-MEM (4 mL/rabbit) and 100 mL seeded on to dentine discs in 96-well plates. Discs were rinsed in PBS 90 min after seeding the cells and then cultured in fresh a-MEM for 48 h. Cells were then fixed in 4% formaldehyde, and the number of osteoclasts, number of F-actin rings, and resorption pit area determined as previously described.[39] In experiments for assessment of effects on prenylation, cultures of pure rabbit osteoclasts in 12-well plates were also generated by incubating marrow cells isolated from long bones of neonatal

rabbits with 1,25 $(OH)_2D_3$, as previously described,[40] and Western blotted as described above.

Acknowledgment. This research was supported by Procter & Gamble Pharmaceuticals, Inc. C. E. McKenna was a consultant for Procter & Gamble Pharmaceuticals, Inc. to 12/2008, during which period some of this work was done. K. M. Błażewska was a 2007-9 WiSE Fellow.

Supporting Information Available: NMR spectra of **1**, **3**, and **6**−**15**; HPLC traces for the **1** and **3** enantiomer separations; pH dependence of **3** UV spectrum; synthetic and chiral HPLC separation details for **13**−**15**; stability of **13** to racemization; RGGT inhibition curves for isolated **3**-E1 and E2 adducts. This material is available free of charge via the Internet at http://pubs.acs.org.

References

(1) (a) Ling, Y.; Sahota, G.; Odeh, S.; Chan, J. M. W.; Araujo, F. G.; Moreno, S. N. J.; Oldfield, E. Bisphosphonate inhibitors of *Toxoplasma gondi* growth: In vitro, QSAR, and in vivo investigations. *J. Med. Chem.* **2005**, *48*, 3130–3140. (b) Papapoulos, S. E. Bisphosphonate actions: physical chemistry revisited. *Bone* **2006**, *38*, 613–616. (c) Ling, Y.; Li, Z. H.; Miranda, K.; Oldfield, E.; Moreno, S. N. J. The farnesyl-diphosphate/geranylgeranyl-diphosphate synthase of Toxoplasma gondii is a bifunctional enzyme and a molecular target of bisphosphonates. *J. Biol. Chem.* **2007**, *282*, 30804–30816. (d) Kotsikorou, E.; Song, Y. C.; Chan, J. M. W.; Faelens, S.; Tovian, Z.; Broderick, E.; Bakalara, N.; Docampo, R.; Oldfield, E. Bisphosphonate inhibition of the exopolyphosphatase activity of the Trypanosoma brucei soluble vacuolar pyrophosphatase. *J. Med. Chem.* **2005**, *48*, 6128–6139. (e) Zhang, Y.; Leon, A.; Song, Y.; Studer, D.; Haase, C.; Koscielski, L. A.; Oldfield, E. Activity of nitrogen-containing and non-nitrogen-containing bisphosphonates on tumor cell lines. *J. Med. Chem.* **2006**, *49*, 5804–5814. (f) Roelofs, A. J.; Thompson, K.; Gordon, S.; Rogers, M. J. Molecular mechanisms of action of bisphosphonates: current status. *Clin. Cancer Res.* **2006**, *12*, 6222S–6230S. (g) Russell, R. G. G.; Watts, N. B.; Ebetino, F. H.; Rogers, M. J. Mechanisms of action of bisphosphonates: similarities and differences and their potential influence on clinical efficacy. *Osteoporosis Int.* **2008**, *19*, 733–759. (h) Dunford, J. E.; Kwaasi, A. A.; Rogers, M. J.; Barnett, B. L.; Ebetino, F. H.; Russell, R. G. G.; Oppermann, U.; Kavanagh, K. L. Structure−activity relationships among the nitrogen containing bisphosphonates in clinical use and other analogues: time-dependent inhibition of human farnesyl pyrophosphate synthase. *J. Med. Chem.* **2008**, *51*, 2187–2195. (i) Nancollas, G. H.; Tang, R.; Phipps, R. J.; Henneman, Z.; Gulde, S.; Wu, W.; Mangood, A.; Russell, R. G. G.; Ebetino, F. H. Novel insights into actions of bisphosphonates on bone: differences in interactions with hydroxyapatite. *Bone* **2006**, *38*, 617–627. (j) Peng, Z.-Y.; Mansour, J. M.; Araujo, F.; Ju, J.-Y.; McKenna, C. E.; Mansour, T. E. Some phosphonic acid analogs as inhibitors of pyrophosphate-dependent phosphofructokinase, a novel target in *Toxoplasma gondii*. *Biochem. Pharm.* **1995**, *49*, 105–113.

(2) Russell, R. G. G.; Xia, Z.; Dunford, J. E.; Oppermann, U.; Kwaasi, A.; Hulley, P. A.; Kavanagh, K. L.; Triffitt, J. T.; Lundy, M. W.; Phipps, R. J.; Barnett, B. L.; Coxon, F. P.; Rogers, M. J.; Watts, N. B.; Ebetino, F. H. Bisphosphonates−an update on mechanisms of action and how these relate to clinical efficacy. *Skeletal Biol. Med., Part B* **2007**, *1117*, 209–257.

(3) Coxon, F. P.; Helfrich, M. H.; Larijani, B.; Muzylak, M.; Dunford, J. E.; Marshall, D.; McKinnon, A. D.; Nesbitt, S. A.; Horton, M. A.; Seabra, M. C.; Ebetino, F. H.; Rogers, M. J. Identification of a novel phosphonocarboxylate inhibitor of Rab geranylgeranyl transferase that specifically prevents Rab prenylation in osteoclasts and macrophages. *J. Biol. Chem.* **2001**, *276*, 48213–48222.

(4) Roelofs, A. J.; Hulley, P. A.; Meijer, A.; Ebetino, F. H.; Graham, R.; Russell, G.; Shipman, C. M. Selective inhibition of Rab prenylation by a phosphonocarboxylate analogue of risedronate induces apoptosis, but not S-phase arrest, in human myeloma cells. *Int. J. Cancer* **2006**, *119*, 1254–1261.

(5) Coxon, F. P.; Ebetino, F. H.; Mules, E. H.; Seabra, M. C.; McKenna, C. E.; Rogers, M. J. Phosphonocarboxylate inhibitors of Rab geranylgeranyl transferase disrupt the prenylation and membrane localization of Rab proteins in osteoclasts in vitro and in vivo. *Bone* **2005**, *37*, 349–358.

(6) Cheng, K. W.; Lahad, J. P.; Gray, J. W.; Mills, G. B. Emerging role of RAB GTPases in cancer and human disease. *Cancer Res.* **2005**, *65*, 2516–2519.

(7) (a) Pereira-Leal, J. B.; Seabra, M. C. The mammalian Rab family of small GTPases: definition of family and subfamily sequence motifs suggests a mechanism for functional specificity in the Ras superfamily. *J. Mol. Biol.* **2000**, *301*, 1077–1087. (b) Leung, K. F.; Baron, R.; Seabra, M. C. Geranylgeranylation of Rab GTPases. *J. Lipid Res.* **2006**, *47*, 467–475.

(8) Marma, M. S.; Xia, Z. D.; Stewart, C.; Coxon, F.; Dunford, J. E.; Baron, R.; Kashemirov, B. A.; Ebetino, F. H.; Triffitt, J. T.; Russell, R. G. G.; McKenna, C. E. Synthesis and biological evaluation of alpha-halogenated bisphosphonate and phosphonocarboxylate analogues of risedronate. *J. Med. Chem.* **2007**, *50*, 5967–5975.

(9) Blazewska, K. M.; Kashemirov, B. A.; Stewart, C. A.; Coxon, F. P.; Baron, R.; Rogers, M. J.; Seabra, M. C.; Ebetino, F. H.; McKenna, C. E. 42nd Western Regional Meeting of the American Chemical Society, Las Vegas, NV, Sept 23−27, 2008; Abstract WRM-070.

(10) (a) Cheng, K. W.; Lahad, J. P.; Kuo, W. L.; Lapuk, A.; Yamada, K.; Auersperg, N.; Liu, J. S.; Smith-McCune, K.; Lu, K. H.; Fishman, D.; Gray, J. W.; Mills, G. B. The RAB25 small GTPase determines aggressiveness of ovarian and breast cancers. *Nat. Med.* **2004**, *10*, 1251–1256. (b) Gebhardt, C.; Breitenbach, U.; Richter, K. H.; Furstenberger, G.; Mauch, C.; Angel, P.; Hess, J. C-fos-dependent induction of the small ras-related GTPase Rab11a in skin carcinogenesis. *Am. J. Pathol.* **2005**, *167*, 243–253.

(11) Lackner, M. R.; Kindt, R. M.; Carroll, P. M.; Brown, K.; Cancilla, M. R.; Chen, C. Y.; de Silva, H.; Franke, Y.; Guan, B.; Heuer, T.; Hung, T.; Keegan, K.; Lee, J. M.; Manne, V.; O'Brien, C.; Parry, D.; Perez-Villar, J. J.; Reddy, R. K.; Xiao, H. J.; Zhan, H. J.; Cockett, M.; Plowman, G.; Fitzgerald, K.; Costa, M.; Ross-Macdonald, P. Chemical genetics identifies Rab geranylgeranyl transferase as an apoptotic target of farnesyl transferase inhibitors. *Cancer Cell* **2005**, *7*, 325–336.

(12) (a) Watanabe, M.; Fiji, H. D. G.; Guo, L.; Chan, L.; Kinderman, S. S.; Slamon, D. J.; Kwon, O.; Tamanoi, F. Inhibitors of protein geranylgeranyltransferase I and Rab geranylgeranyltransferase identified from a library of allenoate-derived compounds. *J. Biol. Chem.* **2008**, *283*, 9571–9579. (b) Guo, Z.; Wu, Y. W.; Tan, K. T.; Bon, R. S.; Guiu-Rozas, E.; Delon, C.; Nguyen, U. T.; Wetzel, S.; Arndt, S.; Goody, R. S.; Blankenfeldt, W.; Alexandrov, K.; Waldmann, H. Development of selective RabGGTase inhibitors and crystal structure of a RabGGTase−inhibitor complex. *Angew. Chem., Int. Ed.* **2008**, *47*, 3747–3750.

(13) Boissier, S.; Ferreras, M.; Peyruchaud, O.; Magnetto, S.; Ebetino, F. H.; Colombel, M.; Delmas, P.; Delaisse, J.-M.; Clezardin, P. Bisphosphonates inhibit breast and prostate carcinoma cell invasion, an early event in the formation of bone metastases. *Cancer Res.* **2000**, *60*, 2949–2954.

(14) Fournier, P. G. J.; Dauhine, F.; Lundy, M. W.; Rogers, M. J.; Ebetino, F. H.; Clezardin, P. Lowering Bone Mineral Affinity of Bisphosphonates as a Therapeutic Strategy to Optimize Skeletal Tumor Growth Inhibition In Vivo. *Cancer Res.* **2008**, *68*, 8945–8953.

(15) Takeuchi, M.; Sakamoto, S.; Kawamuki, K.; Kurihara, H.; Nakahara, H.; Isomura, Y. Studies on novel bone resorption inhibitors. II. Synthesis and pharmacological activities of fused aza-heteroarylbisphosphonate derivatives. *Chem. Pharm. Bull.* **1998**, *46*, 1703–1709.

(16) (a) Kashemirov, B. A.; Marma, M. S.; Mallard, I.; Ebetino, F. H.; Coxon, F. P.; Rojas, J.; Rogers, M. J.; McKenna, C. E. 16th International Conference on Phosphorus Chemistry, Birmingham, UK, July 4−9, 2004; Abstract PS2−041. (b) Bala, J.; Mallard, I.; Kashemirov, B. A.; Coxon, F. P.; Rogers, M J.; Ebetino, F. H.; McKenna, C. E. 40th Western Regional Meeting of the American Chemical Society, Anaheim, CA USA, Jan. 22−25 2006; Abstract WRM−129.

(17) Baron, R. A.; Tavare, R.; Figueiredo, A. C.; Blazewska, K. M.; Kashemirov, B. A.; McKenna, C. E.; Ebetino, F. H.; Taylor, A.; Rogers, M. J.; Coxon, F. P.; Seabra, M. C. Phosphonocarboxylates Inhibit the Second Geranylgeranyl Addition by Rab Geranylgeranyl Transferase. *J. Biol. Chem.* **2009**, *284*, 6861–6868.

(18) Ebetino, F. H.; Bayless, A. V.; Dansereau, S. M. Phosphonocarboxylate compounds pharmaceutical compositions, and methods for treating abnormal calcium and phosphate metabolism. U.S. Patent 5,760,021, **1998**.

(19) Almirante, L; Mugnaini, A.; Detoma, N.; Gamba, A.; Murmann, W.; Hidalgo, J. Imidazole Derivatives. 4. Synthesis and Pharmacologic Activity of Oxygenated Derivatives of Imidazo [1,2-*a*]-Pyridine. *J. Med. Chem.* **1970**, *13*, 1048–1051.

(20) Gueiffier, A.; Lhassani, M.; Elhakmaoui, A.; Snoeck, R.; Andrei, G.; Chavignon, O.; Teulade, J. C.; Kerbal, A.; Essassi, E. M.; Debouzy, J. C.; Witvrouw, M.; Blache, Y.; Balzarini, J.; DeClercq,

E.; Chapat, J. P. Synthesis of *acyclo*-C-nucleosides in the imidazo-[1,2-*a*]pyridine and pyrimidine series as antiviral agents. *J. Med. Chem.* **1996**, *39*, 2856–2859.
(21) Hooper, N.; Beeching, L. J.; Dyke, J. M.; Morris, A.; Ogden, J. S.; Dias, A. A.; Costa, M. L.; Barros, M. T.; Cabral, M. H.; Moutinho, A. M. C. A study of the thermal decomposition of 2-azidoethanol and 2-azidoethyl acetate by ultraviolet photoelectron spectroscopy and matrix isolation infrared spectroscopy. *J. Phys. Chem. A* **2002**, *106*, 9968–9975.
(22) Chezal, J. M.; Delmas, G.; Mavel, S.; Elakmaoui, H.; Metin, J.; Diez, A.; Blache, Y.; Gueiffier, A.; Rubiralta, M.; Teulade, J. C.; Chavignon, O. Solid-supported heterocumulenes: preparation and crystal structure of azaaplysinopsins. *J. Org. Chem.* **1997**, *62*, 4085–4087.
(23) Kondo, K.; Morohoshi, S.; Mitsuhashi, M.; Murakami, Y. Synthetic utility of *tert*-butyl azidoacetate on the Hemetsberger–Knittel reaction (synthetic studies of indoles and related compounds part 47). *Chem. Pharm. Bull.* **1999**, *47*, 1227–1231.
(24) (a) Bleicher, K. H.; Gerber, F.; Wuthrich, Y.; Alanine, A.; Capretta, A. Parallel synthesis of substituted imidazoles from 1,2-aminoalcohols. *Tetrahedron Lett.* **2002**, *43*, 7687–7690. (b) Shin, C.; Yonezawa, Y.; Obara, T.; Nishio, H. Dehydrooligopeptides. 8. Convenient Syntheses of Various Dehydrotyrosine Derivatives Protected with Useful N,O-Protecting Groups Via N-Carboxy Dehydrotyrosine Anhydrides. *Bull. Chem. Soc. Jpn.* **1988**, *61*, 885–891.
(25) (a) Pudovik, A. N.; Guryanov, I. V.; Banderov, Lv.; Romanov, G. V. Phosphonate–Phosphate Rearrangement of Esters of Alpha-Hydroxyalkylphosphonic Acids. *J. Gen. Chem. U.S.S.R.* **1968**, *38*, 142–149. (b) Hammerschmidt, F.; Zbiral, E. Novel Synthetic Aspects of the Phosphonate–Phosphate Rearrangement. 2. Synthesis of Enolphosphates from 1-Oxoalkanphosphonates and Sulfur-Ylides. *Monatsh. Chem.* **1980**, *111*, 1015–1023. (c) Hammerschmidt, F. Phosphonate–Phosphate Rearrangement and Phosphate–Phosphonate Rearrangement and Its Application. 2. Stereochemistry of Phosphonate–Phosphate Rearrangement at Carbon as Exemplified by the Isomerization of (R)-(+)-(1-Hydroxy-1-phenylethyl)phosphonic and (S)-(−)-(1-Hydroxy-1-phenylethyl)phosphonic acid diethyl ester. *Monatsh. Chem.* **1993**, *124*, 1063–1069. (d) McKenna, C. E.; Kashemirov, B. A. Recent progress in carbonylphosphonate chemistry. In *New Aspects in Phosphorus Chem. I*; Springer: Heidelberg, Germany, 2002; Vol. 220, pp 201–238. (e) Sanchez, G. V., Jr.; Kashemirov, B. A.; McKenna, C. E. 40th Western Regional Meeting of the American Chemical Society, Anaheim, CA, Jan 22–25, 2006; Abstract WRM-130.
(26) Deprele, S.; Kashemirov, B. A.; Hogan, J. M.; Ebetino, F. H.; Barnett, B. L.; Evdokimov, A.; McKenna, C. E. Farnesyl pyrophosphate synthase enantiospecificity with a chiral risedronate analog, [6,7-dihydro-5*H*-cyclopenta[*c*]pyridin-7yl(hydroxy)methylene]bis-(phosphonic acid) (NE-10501): synthetic, structural, and modeling studies. *Bioorg. Med. Chem. Lett.* **2008**, *18*, 2878–2882.
(27) (a) Lammerhofer, M.; Lindner, W. Quinine and quinidine derivatives as chiral selectors. 1. Brush type chiral stationary phases for high-performance liquid chromatography based on cinchonan carbamates and their application as chiral anion exchangers. *J. Chromatogr., A* **1996**, *741*, 33–48. (b) Maier, N. M.; Nicoletti, L.; Lammerhofer, M.; Lindner, W. Enantioselective anion exchangers based on cinchona alkaloid-derived carbamates: influence of C-8/C-9 stereochemistry on chiral recognition. *Chirality* **1999**, *11*, 522–528.
(28) Dunford, J. E.; Thompson, K.; Coxon, F. P.; Luckman, S. P.; Hahn, F. M.; Poulter, C. D.; Ebetino, F. H.; Rogers, M. J. Structure–activity relationships for inhibition of farnesyl diphosphate synthase in vitro and inhibition of bone resorption in vivo by nitrogen-containing bisphosphonates. *J. Pharmacol. Exp. Ther.* **2001**, *296*, 235–242.
(29) Lerner, E. C.; Qian, Y. M.; Hamilton, A. D.; Sebit, S. M. Disruption of Oncogenic K-RAS4B Processing and Signaling by a Potent Geranylgeranyltransferase-I Inhibitor. *J. Biol. Chem.* **1995**, *270*, 26770–26773.
(30) McGuire, T. F.; Qian, Y. M.; Vogt, A.; Hamilton, A. D.; Sebti, S. M. Platelet-Derived Growth Factor Receptor Tyrosine Phosphorylation Requires Protein Geranylgeranylation But Not Farnesylation. *J. Biol. Chem.* **1996**, *271*, 27402–27407.
(31) Ebetino, F. H.; Bayless, A. V.; Amburgey, J.; Ibbotson, K. J.; Dansereau, S.; Ebrahimpour, A. Elucidation of a pharmacophore for the bisphosphonate mechanism of bone antiresorptive activity. *Phosphorus, Sulfur Silicon Relat. Elem.* **1996**, *110*, 217–220.
(32) Lawson, M. A.; Coulton, L.; Ebetino, F. H.; Vanderkerken, K.; Croucher, P. I. Geranylgeranyl transferase type II inhibition prevents myeloma bone disease. *Biochem. Biophys. Res. Commun.* **2008**, *377*, 453–457.
(33) (a) Kotti, T.; Head, D. D.; McKenna, C. E.; Russell, D. W. Biphasic requirement for geranylgeraniol in hippocampal long-term potentiation. *Proc. Natl. Acad. Sci. U.S.A.* **2008**, *105*, 11394–11399. (b) Tian, X.; Jin, R. U.; Bredemeyer, A. J.; Oates, E. J.; Błażewska, K. M.; McKenna, C. E.; Mills, J. C. RAB26 and RAB3D Are Direct Transcriptional Targets of MIST1 That Regulate Exocrine Granule Maturation. *Mol. Cell Biol.* **2010**, *30*, 1269–1284.
(34) Paudler, W. W.; Blewitt, H. L. NMR Spectra and Pi-Electron Densities of Some Imidazo(1,2-*a*) Pyridines. *Tetrahedron* **1965**, *21*, 353–361.
(35) Błażewska, K. M.; Haiges, R.; Kashemirov, B. A.; Ebetino, F. H.; McKenna, C. E. 18th International Conference on Phosphorus Chemistry, Wrocław, Poland, July 12–15, 2010; *idem*, manuscript in preparation.
(36) Seabra, M. C.; James, G. L. Prenylation assays for small GTPases. *Transmembr. Signal Protoc.* **1998**, *84*, 251–260.
(37) Kavanagh, K. L.; Dunford, J. E.; Bunkoczi, G.; Russell, R. G. G.; Oppermann, U. The crystal structure of human geranylgeranyl pyrophosphate synthase reveals a novel hexameric arrangement and inhibitory product binding. *J. Biol. Chem.* **2006**, *281*, 22004–22012.
(38) Frith, J. C.; Rogers, M. J. Antagonistic effects of different classes of bisphosphonates in osteoclasts and macrophages in vitro. *J. Bone Miner. Res.* **2003**, *18*, 204–212.
(39) Coxon, F. P.; Helfrich, M. H.; Van't Hof, R.; Sebti, S.; Ralston, S. H.; Hamilton, A.; Rogers, M. J. Protein geranylgeranylation is required for osteoclast formation, function, and survival: inhibition by bisphosphonates and GGTI-298. *J. Bone Miner. Res.* **2000**, *15*, 1467–1476.
(40) Coxon, F. P.; Frith, J. C.; Benford, H. L.; Rogers, M. J. Isolation and purification of rabbit osteoclasts. *Bone Res. Protoc.* **2003**, *80*, 89–99.